Response of latticed shell subjected to uniform and spatially varying spectrum-matched seismic ground motion excitations

X.Z. Cui
Assistant Professor, School of Civil and Environmental Engineering, Harbin Institute of Technology, Shenzhen, China. Email: cuixizhong@hit.edu.cn

X.H. Jiang
Ph.D. Student, Department of Civil and Environmental Engineering, University of Western Ontario, London, Canada. Email: xjian257@uwo.ca

H.P. Hong
Professor, Department of Civil and Environmental Engineering, University of Western Ontario, London, Canada. Email: hhong@uwo.ca

ABSTRACT: Seismic design of latticed shell structures requires the use of structural analysis results obtained by using the design spectrum-matched ground motion records. As finding such records from the database of the actual recorded ground motions is often difficult, synthetic spectrum-matched ground motions are often employed. It is noted that for large span structures such as lattice shells, each of its supports could experience (partially) time-frequency dependent coherent ground motion excitations, including the wave passage effects. The partially coherent and spatially varying spectrum-matched ground motions may influence the peak seismic responses. However, the investigation of such an influence has not been investigated. This is partly due to the unavailability of a popular algorithm to sample such spectrum-matched records.

In the present study, an algorithm to simulate spatially varying spectrum-matched ground motions is proposed based on Fourier transform and S transform (ST). The proposed algorithm iteratively edits the ST coefficient. It also involves the use of a recently developed iterative power and amplitude correction (IPAC) algorithm that is capable of generating multivariate (partially) coherent nonstationary non-Gaussian processes. The use of the proposed algorithm results in simulated records that match the prescribed design spectra and coherence function. Sets of spatially varying spectrum-matched records are simulated and used to assess the seismic response of a latticed spherical shell. The obtained results are compared with those obtained by considering fully coherent spectrum-matched records. The comparison indicates that the consideration of spectrum-matched records with prescribed time and spatially varying characteristics can influence the seismic peak response of latticed spherical shell. This implies one may need to consider such an influence for the seismic design of large-span latticed structures.

1. INTRODUCTION

The assessment of the structural nonlinear dynamic response subjected to the seismic loading forms a crucial step in designing new and evaluating existing structures. The selection of ground motions from the database of actual recorded ground motions that are compatible with a set of prescribed criteria and design response spectrum at a site is always a challenging task (Hancock et al. 2006; Suarez and Montejo 2007; Lancieri et al. 2018). This task becomes even more difficult if the seismic analysis and design of large-span structures with multiple supports, such as latticed shell structures, is of interest. This is because the seismic ground motions are spatially varying and (partially) coherent which could be important for seismic responses for a class of structures (Zerva 2009), and the actual ground motion records at multiple spatially distributed locations that exactly match the layout of structural supports are almost no existent. To overcome this record selection problem, the use of simulated ground motion records that satisfy a set of prescribed criteria, including the prescribed design spectrum, could be considered.

It is noted that the algorithms available in the literature are mainly focused on generating the spectrum-matched record for a single site or support (Hancock et al. 2006; Suarez and Montejo 2007; Ni et al. 2013; Li et al. 2016; Mo et. al 2022). The generation of spatially varying spectrum-matched records was presented in Cacciola and Deodatis (2011) and Shields (2015). The approach proposed in Cacciola and Deodatis (2011) assumes that the spectrum-matched ground motion can be constructed by the superposition of a real ground motion record and a correcting process. The approach proposed by Shields (2015) to sample the spectrum-matched ground motions at multiple sites is carried out by iteratively updating the evolutionary power spectral density (EPSD) function that matches the prescribed response spectrum and coherence through random functional perturbations. It was observed that this algorithm could lead to large variability at lower frequencies although the precise reason is unknown. However, it seems that the consideration of time-dependent coherence between ground motions has not been considered in the literature for generating spectrum-matched records. The possible time-dependent coherence between the seismic ground motions was stressed and shown in Cui and Hong (2021) using the results obtained from actual closely spaced ground motion records.

One of the structural types with large-span and multiple supports is the reticulated domes. This structural type is widely used because of its lightweight. The seismic design of this structural type of structure in China is governed by the seismic design spectrum stipulation in GB50011 (2010). The ordinates of the design spectrum are determined based on the code-specified frequent earthquake and rare earthquakes. An assessment of the statistics of the seismic responses of latticed spherical dome subjected to the spectrum-matched records was presented by Hong and Li (2022). However, the spectrum-matched records at different supports were generated by assuming that the records are fully coherent although the wave passage effect was included. Moreover, it was noted that a comparison of the seismic response of a reticulated dome subjected to stochastic uniform and spatially correlated and coherent multiple-support excitation for a scenario seismic event was presented in the literature (Ye et al. 2011; Li et al. 2020), although in such a case the spectrum-matching aspect was not considered. In all cases, a comparison of the seismic responses of the reticulated dome subjected to the ground motions with time-dependent coherence and with time-independent coherence was not reported in the literature.

In the present study, first, a new algorithm is proposed to generate spatially varying spectrum-matched ground motions. The algorithm starts by using a set of records that match the prescribed time-dependent (or time-independent) coherence for the spatially distributed multiple supports as the seed records. The algorithm uses ST for the time-frequency decomposition of the records, and iteratively edits the ST coefficient for spectrum-matching. Numerical examples are employed to show the effectiveness of the algorithm. The sampled spectrum-matched records at multiple supports are then used for evaluating the seismic response of a latticed spherical shell, showing the importance of considering the time-dependent coherence in assessing the seismic response of a large-span lattice dome with multiple supports.

In the following, we first describe the proposed algorithm for generating spectrum-matched records at multiple supports with prescribed design spectrum and spatial coherence. In particular, we illustrate the algorithm for generating the spectrum-matched records by considering the geometry of multiple supports of a lattice spherical shell. We then carry out structural analysis for the considered shell subjected to the seismic excitation defined by the spectrum-matched records.

2. PROPOSED ALGORITHM TO GENERATE SPATIALLY VARYING SPECTRUM-MATCHED GROUND MOTIONS

2.1. Transforms used for processing the record and the proposed algorithm

Consider a structure with n spatially distributed supports. Let $x_z(k\Delta_t)$ denote the digitized ground motions at the z-th support at time $k\Delta_t$, where $z = 1, \ldots, n$, $k = 1, \ldots, N$ and Δ_t is the time increment. The discrete Fourier transform (DFT) of $x_z(k\Delta_t)$ is defined as,

$$\hat{x}_z(p\Delta_f) = FT(x_z(k\Delta_t)) = \sum_{k=1}^{N} x_z(k\Delta_t) e^{-i2\pi pk/N_f} \Delta_t \quad (1)$$

$$x_z(k\Delta_t) = IFT(\hat{x}_z(p\Delta_f)) = \sum_{p=-N/2+1}^{N/2} \hat{x}_z(p\Delta_f) e^{i2\pi pk/N_f} \Delta_f \quad (2)$$

where FT and IFT denote DFT and inverse DFT (IDFT) operation; $\hat{x}(p\Delta_f)$ is the DFT coefficients; $\Delta_f = 1/(\Delta_t N_f)$, N_f represents the number of the frequency points for both positive and negative frequencies, and $N_f\Delta_f = 1/\Delta_t$.

DFT is a non-redundant transform and could provide perfect reconstruction. In the Fourier domain, the transform provides the frequency content of the signal but does not provide time localization information. To gain the time localization information while maintaining the same frequency and phase interpretation as that given by Fourier transform in the transform domain, one could use the S transform (ST) (Stockwell et al. 1996). ST pair for the discretized signal $x_z(k\Delta_t)$ can be written as (Yan and Zhu 2011; Hong and Cui 2020),

$$\begin{aligned} x_{s,z}(p\Delta_f, q\Delta_t) &= ST(x_z(k\Delta_t), p\Delta_f) \\ &= \Delta_f \sum_{j=-N_f/2+1}^{N_f/2} \left[\hat{x}_z\left((j+p)\Delta_f\right) \exp\left(-2\pi^2 j^2/p^2\right) \right] e^{i\frac{2\pi jq}{N_f}} \end{aligned} \quad (3)$$

$$\begin{aligned} x_z(k\Delta_t) &= IST(x_{s,z}(p\Delta_f, q\Delta_t)) \\ &= IFT(\hat{x}_z(p\Delta_f)) \quad p = -N_f/2+1, \cdots, N_f/2 \end{aligned} \quad (4)$$

where $ST(\ )$ and $IST(\ )$ denote the forward and backward ST operators, $q = 1$ to N representing the time index. Eq. (4) is based on the fact that the summation of the ST coefficients, $x_{s,z}(p\Delta_f, q\Delta_t)$, equals FT coefficient (Stockwell et al. 1996),

$$\hat{x}_z(p\Delta_f) = \sum_{q=1}^{N} x_{s,z}(p\Delta_f, q\Delta_t)\Delta_t \quad (5)$$

For example, consider the ground motion record shown in Figure 1a. The calculated Fourier amplitude spectrum and the amplitude of ST coefficients are shown in Figures 1b and 1c. The former provides only frequency dependent information while the latter gives the time and frequency dependent characteristics.

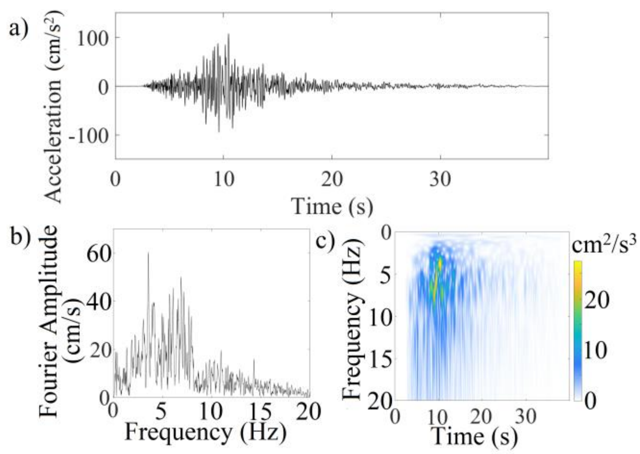

Figure 1: a) Considered ground motion (north-south component from Botas station in 1999 Kocaeli Turkey earthquake, with magnitude 6.7 and rupture distance 41 km); b) its Fourier amplitude spectrum; c) its amplitude of ST coefficients.

2.2. Proposed algorithm

Consider the target response spectrum for the ground motion record to be simulated at each support, $R_{T,z}(f(s), \xi)$, is given, where $f(s)$ denotes the natural vibration frequency at the location indexed by $s = 1, \ldots, N_s$. For simplicity, it is assumed that $f(s)$ is co-collocated with some of the frequencies employed in the discretized FT and ST, which are denoted as $m(s)\Delta_f$ and $m(s)$ take an integer value between 0 and $N_f/2$.

Moreover, it is considered that the spatial coherence between two supports with separation Δ is $\Gamma(\Delta)$. Since the set of seed records, $x_z(k\Delta_t)$, that match the layout of considered structural supports is unlikely available, one could use the same seed record for all considered supports to match the target response spectrum at each considered support but without considering coherence. This can be done by using an algorithm available in the literature (see introduction) to obtain the spectrum-matched records, denoted as $x_{M,z}(k\Delta_t)$. We can calculate the time-frequency dependent power spectral density (TFPSD) function of $x_{M,z}(k\Delta_t)$ (at each considered support). Such TFPSD functions for the considered multiple supports are then used as the target TFPSD functions, together with the target coherence function $\Gamma(\Delta)$, for the simulation of coherent records by using SRM (Shinozuka and Deodatis 1996) or TFSRM (Hong and Cui 2020).

The above forms the first stage of the proposed algorithm. It must be noted that the sample records are coherence-matched records and the spectrum-matching aspect may not satisfactory even though the target TFPSD function was employed in the simulation. In the second stage of the proposed algorithm, we use the simulated records in the first stage as the seed records at the multiple supports to simulate the spectrum-matched records. More specifically, the steps in the second stage are as follows:

1. Let $x_{old,z}(k\Delta_t) = x_z(k\Delta_t)$ for $z = 1,\ldots,n$; calculate the ST coefficients of $x_{old,z}(k\Delta_t)$ and obtain its phase $\theta_z\left(p\Delta_f, q\Delta_t\right)$;
2. Calculate $\hat{x}_{F,z}(p\Delta_f) = FT(x_{old,z}(k\Delta_t))$. Evaluate $R_{A,z}\left(m(s)\Delta_f, \xi\right)$ of $x_{old,z}(k\Delta_t)$ for each considered frequency $m(s)\Delta_f$, and collect the time $n_z(s)\Delta_t$ that the spectral response occurs to form $\left(m(s)\Delta_f, n_z(s)\Delta_t\right)$.
3. Calculate $R_{s,z}\left(m(s)\Delta_f, \xi\right) = \dfrac{R_{T,z}\left(m(s)\Delta_f, \xi\right)}{R_{A,z}\left(m(s)\Delta_f, \xi\right)}$ for $s = 1, \ldots, N_s$;

3.1 Calculate

$R_{field,z}(p\Delta_f, q\Delta_t) = \prod_s r(p\Delta_f, q\Delta_t; m(s)\Delta_f, n_z(s)\Delta_t, R_{s,z}(m(s)\Delta_f, \xi))$, and the function r is defined as,

$$r(f,t;f_0,t_0,r_s) = \begin{cases} 1+\left(r_s-1\right)\left(1-\left|\dfrac{|f|-f_0}{\Delta_{Hf}}\right|^{\alpha_f}\right)\left(1-\left|\dfrac{t-t_0}{\Delta_{Ht}}\right|^{\alpha_t}\right), & \text{for } \left|\dfrac{|f|-f_0}{\Delta_{Hf}}\right| \le 1 \text{ and } \left|\dfrac{t-t_0}{\Delta_{Ht}}\right| \le 1 \\ 1 & \text{otherwise} \end{cases} \tag{6}$$

find frequency h_l (l = 1, 2,…, M) that $\sum_{z=1}^{n}\sum_{q=1}^{N} R_{field,z}(h_l\Delta_f, q\Delta_T) \neq nN$, where M is the total number of found h_l; calculate the ST coefficient at the frequency $h_l\Delta_f$, $\hat{x}_{s,old,l}(h_l\Delta_f, q\Delta_t)$;

3.2 $\hat{x}_{s,new,z}(h_l\Delta_f, q\Delta_t) = \hat{x}_{s,old,z}(h_l\Delta_f, q\Delta_t) \times R_{field,z}(h_l\Delta_f, q\Delta_T)$; update the FT coefficients at frequency $h_l\Delta_f$, $\hat{x}_{F,z}(h_l\Delta_f) = \sum_{q=1}^{N}\hat{x}_{s,new,z}(h_l\Delta_f, q\Delta_t)$; assign $\hat{x}_{F,z}(-h_l\Delta_f) = \hat{x}_{F,z}(h_l\Delta_f)$, and apply $IFT\left(\hat{x}_{F,z}(p\Delta_f)\right)$ to obtain $x_{new,z}(k\Delta_t)$;

3.3 Calculate the ST coefficient of $x_{new,z}(k\Delta_t)$, denoted as $\hat{x}_{s,new,z}(p\Delta_f, q\Delta_t)$, and its phases $\phi_z\left(p\Delta_f, q\Delta_t\right)$. Calculate $\alpha(h_l\Delta_f, q\Delta_t) = \tan^{-1}\left[\dfrac{\sum_{z=1}^{n}\sin\left(\theta_z\left(h_l\Delta_f, q\Delta_t\right) - \phi_z\left(h_l\Delta_f, q\Delta_t\right)\right)}{\sum_{z=1}^{n}\cos\left(\theta_z\left(h_l\Delta_f, q\Delta_t\right) - \phi_z\left(h_l\Delta_f, q\Delta_t\right)\right)}\right]$,

3.4 Update the ST coefficient $\hat{x}_{s,new,z}(p\Delta_f, q\Delta_t) = \left|\hat{x}_{s,new,z}(p\Delta_f, q\Delta_t)\right| e^{i\left[\theta z\left(p\Delta_f, q\Delta_t\right) + \alpha\left(p\Delta_f, q\Delta_t\right)\right]}$, calculate FT coefficient $\hat{x}_{F,z}(p\Delta_f) = \sum_{q=1}^{N}\hat{x}_{s,new,z}(p\Delta_f, q\Delta_t)$, assign $\hat{x}_{F,z}(-p\Delta_f) = \hat{x}_{F,z}(p\Delta_f)$, and apply $IFT\left(\hat{x}_{F,z}(p\Delta_f)\right)$ to obtain $x_{new,z}(k\Delta_t)$;

4. Calculate $R_{A,z}\left(m(s)\Delta_f, \xi\right)$ of $x_{new,z}(k\Delta_t)$ and collect $\left(m(s)\Delta_f, n_z(s)\Delta_t\right)$. If

$$\max\left[\frac{\left|R_{T,z}\left(m(s)\Delta_f,\xi\right)-R_{A,z}\left(m(s)\Delta_f,\xi\right)\right|}{R_{T,z}\left(m(s)\Delta_f,\xi\right)}\right]>\varepsilon \text{ for all } s \text{ and } l \tag{7}$$

where ε is a small specified tolerance value, the convergence is not achieved. Let $x_{old,z}(k\Delta_t)$ $= x_{new,z}(k\Delta_t)$, and repeat Steps 2) to 5);

5. Once convergence is achieved, $x_{new,z}(k\Delta_t)$ is used as the spectrum-matched record.

3. SIMULATED OF RESPONSE SPECTRUM AND COHERENCE MATCHED RECORDS AT MULTIPLE SUPPORT OF A LATTICED SPHERICAL SHELL

3.1. *Considered lattice structure*

For the numerical simulation of the spectrum- and coherence-matched records by using the proposed algorithm, consider the lattice spherical shell shown in Figure 2. Such type of shell with a large-span is often used for sports stadiums, gymnasiums, and auditoriums because of its lightweight. The shell illustrated in Figure 2 is known as a single-layer Kiewit 8 spherical reticulated dome. The dome has a diameter of 120 m, and the height to diameter ratio is 1/5. The geometry of the considered latticed spherical dome is shown in Figure 2a, and the material and geometric properties of the structural members can be found in Table 1. The layout of the supports of the dome is shown in Figure 2b. The dome with 289 joints and 800 members is pinned at the ground level and is modelled in ANSYS® Multiphysics 10.0 (2005), as described in Li and Hong (2020). The cross-sectional properties of the structural steel members are the same for the radial and ring members and are the same for the oblique members. The former and latter are referred to as the structural member Type 1 and Type 2, respectively, in the following. The natural vibration frequencies of the considered dome for the first 500 vibration models are given in Figure 2c. For more details about the finite element modelling in ANSYS, the readers are referred to Li et al. (2020).

Table 1: Geometric and material properties of the structural members of the dome.

Member	*Size*
Radial member	*ϕ325 ×16 mm*
Ring member	*ϕ3325 ×16 mm*
Oblique member	*ϕ273 ×14 mm*
Ring beam	*ϕ1235 ×30 mm*
Column	*1250 N/m2*
Permanent load	*2.06 ×105 N/mm2*
Elasticity modulus	*7850 kg/m3*
Density	*0.3*
Poisson’s ratio	*ϕ325 ×16 mm*

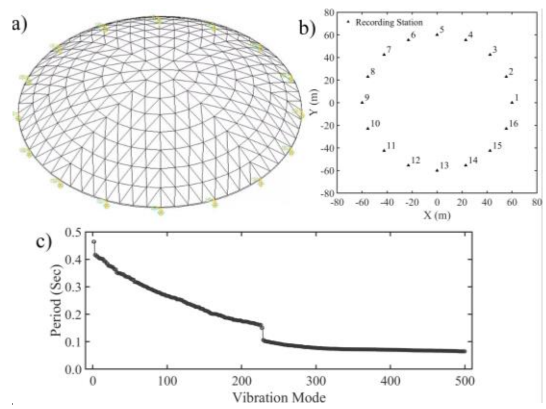

Figure 2: a) Spherical dome b) layout of the supports and c) distribution of natural vibration period.

3.2. *Simulation of the records using the proposed algorithm*

It is considered that the structure shown in Figure 2 is located in a “seismic fortification intensity” zone equal to eight; the specified (effective) PGA value (i.e., 0.45a$_{max}g$) equal to 70 cm/s^2, for the “frequent earthquake” (Li and Hong 2020). The design spectrum for 2% damping, according to GB50011 (2010) and JGJ7 (2010), for the considered structure is shown in Figure 3.

The ground motion record shown in Figure 1a is used as the seed record. 35 discrete frequency points between 0.5 Hz and 20 Hz (period from 0.05 s to 2 s) are selected and the PSA is to be matched at these frequency points. The corresponding period points are also indicated in

Figure 3.

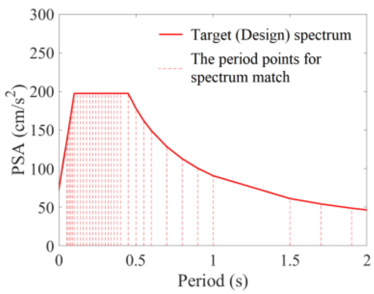

Figure 3: Target design spectrum

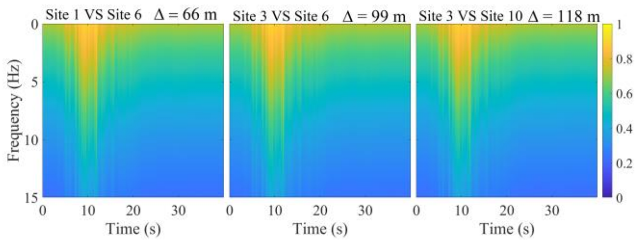

Figure 4: Target coherence for three pairs of supports by considering

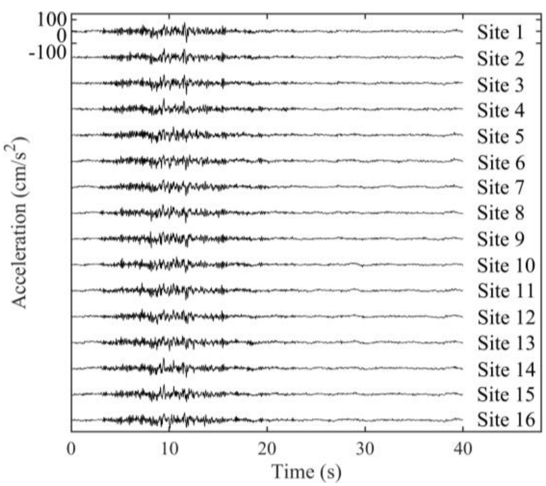

Figure 5: A set of simulated spectrum matched record

To model the spatially varying characteristics of the ground motions, the time-dependent lagged coherence model proposed by Cui and Hong (2021) is adopted in the simulation. An illustration of using this model that is a function of separation Δ, frequency, and intensity of the ground motion is depicted in Figure 4 for three considered pairs of the considered structure sites.

By using the proposed algorithm, a set of the generated spectrum- and coherence-matched records are shown in Figure 5. By repeating the simulation analysis, a total of 25 sets of the spectrum- and coherence-matched ground motion records are generated. The pseudo-spectral acceleration (PSA) of each simulated record at three sites is calculated and shown in Figure 6 and compared to the target, indicating that they match the target well. The coherence for three selected pairs of sites is also calculated for each set of simulated records. The mean of the coherence based on the 25 sets of sampled record are shown in Figure 7. A comparison of the results depicted in Figures 4 and 7 indicates that they agree adequately, especially for a time-frequency region with high excitation intensity.

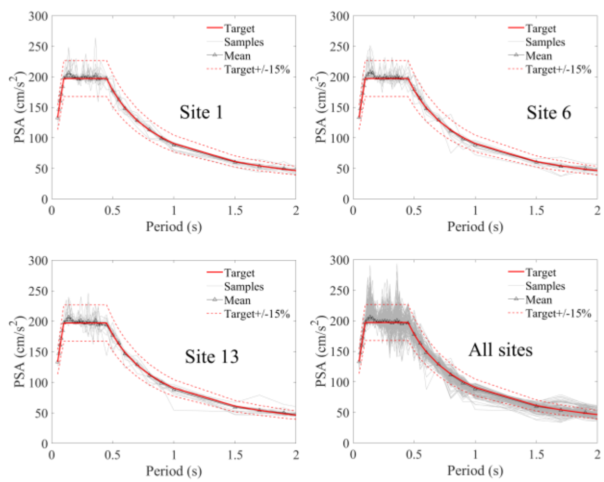

Figure 6: PSA of simulated spectrum-matched records at 3 sites and all sites.

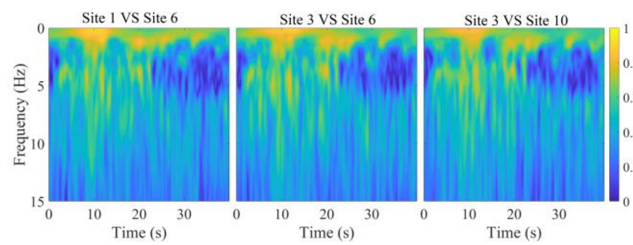

Figure 7: Mean of lagged coherence for three selected pairs of sites calculated using 25 sets of sampled records

4. COMPARISON OF SEISMIC RESPONSE SUBJECTED TO UNIFORM AND NON-UNIFORM GROUND MOTIONS

To see the influence of spatial coherence on the structural responses by considering spectrum matched records, we consider the following two excitation cases:

Uniform spectrum-matched excitation case (U-case): In this case, it is considered that the excitation at all 16 supports is identical to the simulated record at support 1, except that the wave passage effect is included by assuming an apparent velocity equal 1500 m/s and propagating along the X direction shown in Figure 2b. The inclusion of the wave passage effect in the simulated records is carried out using the approach described in Der Kiureghian (1996);
Spatially varying spectrum- and coherence-matched excitation case (S-case): In this non-uniform excitation case, the simulated spectrum- and coherence-matched records at each support are employed. In addition, similar to U-case, the wave passage effect is included.

Structural analysis is carried out by using the 25 sets of records for both U-case and S-case. The maximum values of the responses that are important for structural design and evaluation are extracted for each considered case and each set of simulated records. The considered responses are:

D_T the absolute value of the displacement at the top of the structure;

D the maximum absolute value of time history of displacement of a node considering all node;

A_{F1} the maximum absolute value of time history of the axial force in an element considering all radial and ring members;

A_{F2} the maximum absolute value of time history of the axial force in an element considering all oblique members;

S_{BS} maximum absolute value of the reacting base shear along the direction of excitation at the reference point;

S_{BT} the maximum absolute value of the total base shear along the direction of excitation.

By applying the 25 sets of generated spectrum-matched records based on the seed record shown in Figure 1 to the structures, the values of the 6 parameters for each case are obtained. Their cumulative distribution functions (CDF) are shown in Figure 8. As observed from Figure 8, the maximum displacement and internal force differ by considering uniform or spatially varying excitations. Although the dome subjected to spatially varying excitation leads to a small maximum displacement at the top of the structure, it causes a large maximum displacement by considering all the nodes. Moreover, a significant increase in the internal force including the base shear S_{BS} and axial forces A_{F1} and A_{F2} if non-uniform excitation is considered. These observations suggest that the consideration of time-frequency-dependent coherence could be important in evaluating seismic response for seismic design. This conclusion must be verified further by considering additional structures and seismic design considerations.

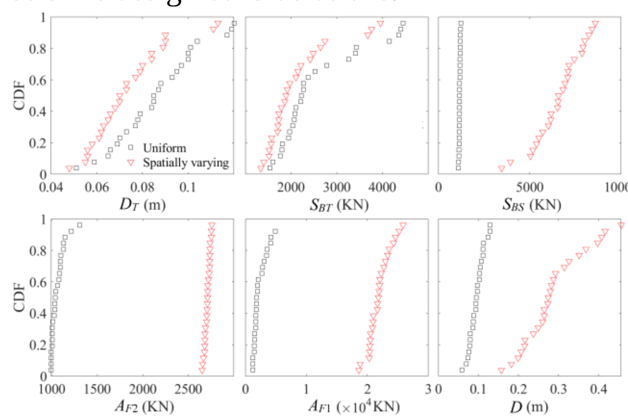

Figure 8: Cumulative distribution function of obtained structural responses.

5. CONCLUSIONS

An iterative algorithm to simulate spatially varying spectrum-matched ground motions with time-dependent coherent characteristics is proposed based on Fourier transform and S transform (ST). The proposed algorithm could adjust the records at each site to match the target design spectra while retaining the time-dependent coherence characteristics.

Numerical analysis using the proposed algorithm is carried out by sampling sets of the spectrum- and coherence-matched records by considering the multiple supports of a latticed spherical shell. The results indicate the adequacy of the proposed algorithm. Using sampled records, seismic analyses of the lattice structure are carried out. The results indicate that the consideration of the time-frequency dependent coherence could be important in evaluating seismic response for seismic design. Since only a single structure is considered, such an important observation must be verified by considering additional structures.

6. ACKNOWLEDGEMENT

We gratefully acknowledge the financial support received from the Harbin Institute of Technology, Western University, and the Natural Sciences and Engineering Research Council of Canada (RGPIN-2016-04814, for HPH).

7. REFERENCES

Cacciola, P., & Deodatis, G. (2011). A method for generating fully non-stationary and spectrum-compatible ground motion vector processes. Soil Dynamics and Earthquake Engineering, 31(3), 351-360.

Cui, X. Z., & Hong, H. P. (2021). A time‐frequency dependent coherence model for seismic ground motions. Earthquake Engineering & Structural Dynamics, 50(3), 955-973.

Deodatis, G. (1996). Non-stationary stochastic vector processes: seismic ground motion applications. Probabilistic engineering mechanics, 11(3), 149-167.

Kiureghian, A. D. (1996). A coherency model for spatially varying ground motions. Earthquake engineering & structural dynamics, 25(1), 99-111.

GB50011. (2010). Code for seismic design of buildings. Beijing: China Architecture & Building Press.

Hancock, J., Watson-Lamprey, J., Abrahamson, N. A., Bommer, J. J., Markatis, A., McCoy, E., & Mendis, R. (2006). An improved method of matching response spectra of recorded earthquake ground motion using wavelets. Journal of earthquake engineering, 10, 67-89.

Hong, H. P., & Cui, X. Z. (2020). Time–frequency spectral representation models to simulate nonstationary processes and their use to generate ground motions. Journal of Engineering Mechanics, 146(9), 04020106.

JGJ7. (2010). Technical specification for space frame structures. Beijing: China Architecture & Building Press. (in Chinese).

Lancieri, M., P. Bazzurro, and O. Scotti. (2018). Spectral matching in time domain: A seismological and engineering analysis. Bulletin of the Seismological Society of America 108 (4): 1972–94.

Li, B., Xie, W. C., & Pandey, M. D. (2016). Generate tri-directional spectra-compatible time histories using HHT method. Nuclear Engineering and Design, 308, 73-85.

Li, Y. G., & Hong, H. P. (2022). Use of spectrum-matched versus scaled records to evaluate seismic responses of a latticed shell. Journal of Earthquake Engineering, 26(8), 4054-4068.

Li, Y. G., Liu, T. J., Fan, F., & Hong, H. P. (2020). Comparison of seismic responses of a reticulated dome under stochastic uniform and spatially correlated and coherent multiple-support excitation for a scenario seismic event. International Journal of Space Structures, 35(4), 113-125.

Mo, H. M., Cui, X. Z., & Hong, H. P. (2022). Generation of spectrum-compatible ground motion records based on time-frequency decomposition. Soil Dynamics and Earthquake Engineering, 161, 107359.

Ni, S. H., Xie, W. C., & Pandey, M. D. (2013). Generation of spectrum-compatible earthquake ground motions considering intrinsic spectral variability using Hilbert–Huang transform. Structural safety, 42, 45-53.

Stockwell, R. G., Mansinha, L., and Lowe, R. P. (1996). Localization of the complex spectrum: the S transform. IEEE Trans. Signal Process., 44(4), 998-1001.

Shields, M. D. (2015). Simulation of spatially correlated nonstationary response spectrum–compatible ground motion time histories. Journal of Engineering Mechanics, 141(6), 04014161.

Suarez, L. E., and L. A. Montejo. (2007). Applications of the wavelet transform in the generation and analysis of spectrum-compatible records. Structural Engineering and Mechanics 27 (2): 173–97.

Shinozuka, M., & Deodatis, G. (1996). Simulation of multi-dimensional Gaussian stochastic fields by spectral representation.

Yan, Y., & H. Zhu. (2011). "The generalization of discrete stockwell transforms." In Proc., 2011 19th IEEE European Signal Processing Conf. IEEE, 1209–1213. New York: IEEE.

Zerva, A. (2009). Spatial variation of seismic ground motions: Modeling and engineering applications, Taylor & Francis, London

Ye, JH, Zhang, ZQ and Chu, Y. (2011) Strength failure of spatial reticulated structures under multi-support excitation. Earthq Eng Eng Vib; 10(1): 21–36.